RSC Advances

COMMUNICATION

View Article Online
View Journal | View Issue

Cite this: *RSC Adv.*, 2016, **6**, 97363

Received 13th September 2016
Accepted 7th October 2016

DOI: 10.1039/c6ra22906a

www.rsc.org/advances

Visible light promoted photocatalytic water oxidation: effect of fluctuating light intensity upon reaction efficiency†

Dominic Walsh,*[a] Pascaline Patureau,[a] Julia Walton,[b] Jason Potticary,[b] Simon R. Hall[b] and Mark T. Weller[a]

Visible light promoted photocatalytic water oxidations were conducted with a synthesized iron oxide nanoparticulate catalyst together with a $[Ru(bpy)_3]^{2+}$ light harvesting dye and electron acceptor. With highest intensity set at daylight equivalent levels, the effects of fluctuating illumination upon ongoing reactions were studied and gaseous O_2 and proton production measured. A light oscillation cycle was identified that significantly increased reaction TOF and quantum yields, which is suggested to arise from improvements in synchronization of the cyclic reaction steps and minimization of light sensitizer self-decomposition.

In tandem with solar photovoltaics, the capture and storage of energy in the form of convenient, inexpensive fuels is an essential goal but remains technically elusive. The design of solar-fuel generation systems with the required efficiency, scalability, and sustainability to be economically viable has clear benefits. Artificial photosynthesis utilizing processes that are akin to Photosystem II (PSII) water oxidation is a vital step towards linking with development of Photosystem I (PSI)-like systems for the complete water splitting reaction and generation of liquid solar fuels.[1–3]

Water oxidation typically utilizes the photocycling light absorbing dye $[Ru(bpy)_3]^{2+}$.[4] The MLCT visible absorption region of the $[Ru(bpy)_3]^{2+}$ light sensitizer ranges from ~420–540 nm (λ_{max} 454 nm) (Fig. 1 inset), hence shorter wavelength visible light is effective in promotion of ruthenium d orbital e^- onto orbitals associated with a bipyridine ligand to give an excited state $Ru(bpy)_3^{2+*}$.

An electron acceptor ($[Co(NH_3)_5Cl]Cl_2$) quenches the excited state $[Ru(bpy)_3]^{2+*}$, giving $[Ru(bpy)_3]^{3+}$.[5] An electron donated from a metal oxide catalyst restores the stable $[Ru(bpy)_3]^{2+}$ state, and absorbed water is oxidized on the metal oxide surface with the release of O_2 gas and protons.[6] In total, 4 photons generate 4 protons and an O_2 molecule.[5,7,8]

$$2H_2O + 4h\nu \rightarrow O_2\uparrow + 4H^+ \text{ (to buffer)} + 4e^- \text{ (to electron acceptor)}$$

Previously we have investigated the effect of catalyst composition and a range of daylight equivalent light intensities at constant levels over a reaction lifetime.[9] Natural daylight intensity levels vary due cloud cover, diurnal, seasonal and other factors and one aim of this research was determine any effect of fluctuating light intensity upon an ongoing reaction profile and yields.

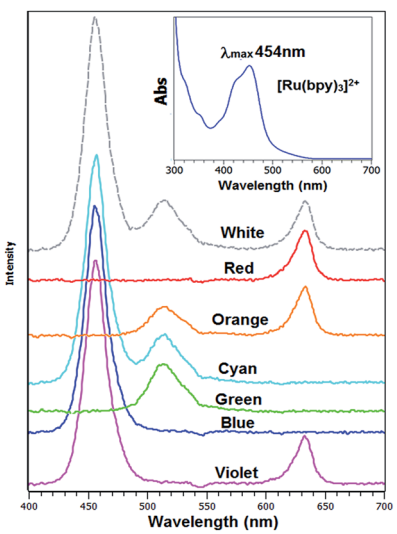

Fig. 1 Graph of RGB led light emissions generated in cyclic colour mode. The blue output was used for continuous light reactions. Yellow/orange through to red light lies at the upper edge or outside the absorption region of $[Ru(bpy)_3]^{2+}$. Inset shows absorption spectrum of $[Ru(bpy)_3]^{2+}$.

[a]*Department of Chemistry, University of Bath, Bath, BA2 7AY, UK. E-mail: walshddr@gmail.com*

[b]*School of Chemistry, University of Bristol, Cantocks Close, Bristol, BS8 1TS, UK*

† Electronic supplementary information (ESI) available: Experimental details and catalyst XRD, TEM, UV-vis spectroscopy and EDX, led emission and O_2 yields under cyclic light and using Co_3O_4 catalyst, FT-IR of decomposed $[Ru(bpy)_3]^{2+}$, example calculations. See DOI: 10.1039/c6ra22906a

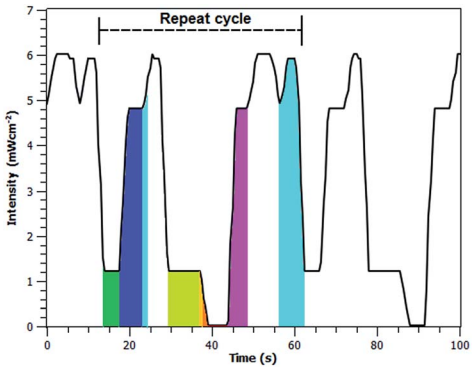

Fig. 2 Measured 50 s cycling light wavelength/intensity at reaction flask over 420–540 nm (matching the $[Ru(bpy)_3]^{2+}$ absorption region). $\bar{x} = 3.3$ mW cm^{-2} and includes 5 s intervals of non-absorbed red light.

A nanoparticulate iron oxide was prepared as an earth abundant non-toxic catalyst component of the photocatalysis reaction.[10,11] The oxide was prepared by simple short and moderate temperature calcining methodology utilizing the natural polymer xyloglucan.[12] This acts as a sacrificial agent to limit particle size during the heating process (catalyst synthesis is described in the ESI†). Powder XRD showed the catalyst to be near pure α-Fe_2O_3 (JCPDS 013-0534-hematite) together with a trace of γ-Fe_2O_3 (JCPDS 024-081, maghemite). TEM showed the presence of irregular nanoparticles of ~10–100 nm in dimension, EDX showed presence of Fe and O only (Fig. S1a–c, ESI†). Brunauer–Emmett–Teller (BET) N_2 adsorption surface area was measured as 36.3 m^2 g^{-1}, with calculated average particle size of ~30 nm. Solid state UV-vis spectroscopy of the Fe_2O_3 was measured and Tauc plots indicated direct and indirect band gaps of 2.02 and 1.88 eV respectively (Fig. S2a–c, ESI†). Nanoparticulate hematite has a reported direct band gap of ~2.2 eV, the presence of trace levels of γ-Fe_2O_3 may promote the red-shift in band-gaps observed.[13]

In situ realtime measurement of O_2 released into the flask headspace by an accurate optical sensor system and proton generation by pH probe measurement was undertaken.[9,14] A RGB led capable of cyclic output and also pure colour led's were utilized as light sources. Measurements were made in triplicate with representative yield profiles shown, full experimental and instrumentation details are described in the ESI.†

Photocatalytic water oxidations of 60 min duration were initially conducted using a standard blue led (λ_{max} 455 nm) source with measured light intensity at the stirred reaction flask at a daylight equivalent level of 5 mW cm^{-2}.[9] This was then compared to reactions conducted with the led source set to a colour spectrum cycle of 25, 50 or 100 s duration repeated for 60 min which generated violet through to red including white by mixing of the RGB led sources. Fig. 1 shows the measured RGB wavelengths and relative intensities.

Fig. 2 shows the actual fluctuating light intensity received at the reaction flask of between 0 to 6 mW cm^{-2} (average of 3.3 mW cm^{-2}) over the $[Ru(bpy)_3]^{2+}$ absorption region, using a 50 s repeat cycle. Finally, comparison was made to a light source using pure colour λ_{max} 410, 450 and 500 nm led sources giving

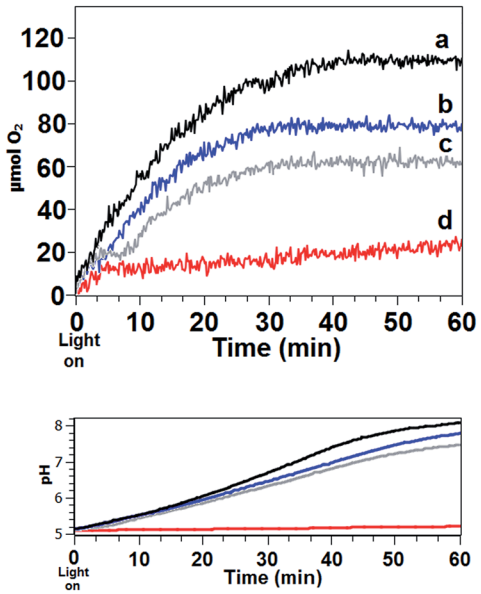

Fig. 3 Graph of released O_2 (μmol) against time for photocatalyzed water oxidation reactions with α-Fe_2O_3 catalyst (10 mg), $[Ru(bpy)_3]^{2+}$ (45 mg) and $[Co(NH_3)_5Cl]Cl_2$ (124 mg) in 35 ml of degassed acetate buffer (pH 5.1, 50 mM) using light source of (a) 50 s cyclic 0–6 mW cm^{-2} ($\bar{x} = 3.3$ mW cm^{-2}); (b) 5 mW cm^{-2} λ 455 nm; (c) 5 mW cm^{-2} λ 400–540 nm and (d) λ 630 nm. Corresponding change in pH with time for these reactions is also shown (pH increase is caused by decomposition of electron acceptor with liberation of ammonia).

a combined continuous illumination of 400–540 nm, to test effects of full saturation of the $[Ru(bpy)_3]^{2+}$ absorption region (Fig. S3, ESI†).

Comparison of measured O_2 yields and reaction rates showed that 50 s cycle gave highest O_2 yield and reaction rate compared to a 25 s and 100 s lighting cycle (Fig. S4, ESI†). As the repeating 50 second duration fluctuating cycle was in the optimal zone it was used for further comparison to continuous illumination reactions.

Fig. 3 shows gaseous O_2 generation for 60 min photoreactions using the reagent mixture in stirred N_2 degassed acetate buffer. Yield profiles for differing lighting conditions including red light as a non-light absorbing control system are shown. Significantly the 50 s cyclic fluctuating illumination gave

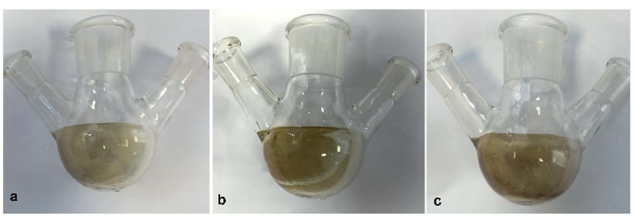

Fig. 4 Images of rinsed reaction flask following photocatalytic water oxidation using illumination of (a) 50 s cyclic; (b) 5 mW cm^{-2} blue (λ_{max} 455 nm) and (c) 5 mW cm^{-2} λ 400–540 nm. A thinner layer of insoluble decomposed $[Ru(bpy)_3]^{2+}$ was obtained with cyclic illumination, whereas saturation of the absorption region resulted in apparent elevated decomposition.

Table 1 Maximum net O_2 generated, calculated TOFs (TOF as mol O_2 per sec per mol (active) metal). Quantum yield $\Phi O_2\% = O_2$ produced at $t = O_2$max @ 40 min per photons absorbed at $t = 40$ min × 400% (4 photons absorbed per O_2). S_{BET}, $m^2\ g^{-1}$ α-$Fe_2O_3 = 36.3$, $Co_3O_4 = 35.8$. (See Fig. 2) (example calculations are shown in the ESI)

Catalyst (10 mg)	Light source (nm)	O_2 yield (at $t = 40$ min) μmol	TOF_{max} ($t = 0$–10 min) $\times 10^{-4}\ s^{-1}$	$\Phi O_2\%$ at $t = 40$ min
α-Fe_2O_3	Cyclic (50 s)	108	7.667	45.6
α-Fe_2O_3	Cyclic (25 s)	69	3.994	29.1
α-Fe_2O_3	Cyclic (100 s)	55	2.394	23.2
α-Fe_2O_3	455	79	4.792	22.0
α-Fe_2O_3	400–540	62	3.195	17.3
α-Fe_2O_3	630	20	0.7987	5.58
Co_3O_4	Cyclic (50 s)	117	10.44	49.4
Co_3O_4	455	75	5.622	20.9

a ~30% increased O_2 yield compared to 5 mW cm^{-2} blue light (Fig. 3a and b). This is despite the overall average illumination being ~30% reduced compared to the continuous blue illumination. Saturation of the absorption region with combined led sources gave further reduced yields compared to both the 50 s cyclic and blue sources (Fig. 3c). Red light (together with a low level of ambient light of intensity 0.1–0.2 mW cm^{-2}) produced almost no reaction (Fig. 3d). Increase in pH due to capture of electrons from Ru-bpy bonding orbitals in the excited state by the pentamine cobalt acceptor and its subsequent decomposition liberating ammonia corresponds to measured O_2 generation profiles (Fig. 3).[5]

To establish if lighting effects are replicated using an alternative system, the photocatalyzed water oxidation was repeated using a commercial Co_3O_4 nanoparticle powder as catalyst, Co_3O_4 is known to be an effective catalyst for water oxidations.[15] Reactions using the 50 s cyclic light were compared to continuous 5 mW cm^{-2} blue illumination, an increase in O_2 yield of ~35% combined with increased TOF was obtained with 50 s cyclic illumination (Fig. S5, ESI†).

The half water splitting reaction is oxidative and thus reagents, in particular organic components are subject to degradation. Cessation of the photocatalytic reaction, which begins after 20–30 min is due to gradual exhaustion of the electron acceptor and also increasing decomposition of the $[Ru(bpy)_3]^{2+}$ dye. In this photoaquation process bipyridine ligands are displaced from the ruthenium and can be observed to form a breakdown product which accumulates as a low solubility dark coloured tar like deposit on the flask surface. Mixture composition is believed to be bipyridine and hydroxylated derivatives of $Ru(bpy)_2^{2+}$.[16–19] An FT-IR comparison of $Ru(bpy)_3Cl_2$ and collected degraded bipyridine material was consistent with the suggested breakdown materials (Fig. S6, ESI†). The relative degradation processes will be the subject of a separate detailed study.

Significantly, examination of rinsed flasks following 60 min of reaction time suggested that levels of adsorbed hydrocarbon breakdown products was reduced when 50 s cyclic illumination was employed compared to continuous illumination (Fig. 4). Catalysis Turn Over Frequencies (TOF's) and quantum yields (Φ) were calculated from O_2 generation rate and yields, light intensity and wavelength and are shown on Table 1.

Overall, continuous blue light illumination was satisfactory however saturation of the $[Ru(bpy)_3]^{2+}$ absorption region in intensity and wavelength was detrimental. Significantly, the results suggest an improved balance between a fluctuating illumination pattern and sufficient generation of the $[Ru(bpy)_3]^{2+*}$ for the cyclic photoreaction exists using a 50 s cycle that includes a ~5 s effective zero illumination zone each cycle.

Water oxidation at the surface of the heterogeneous moderately active iron oxide catalyst is believed to be the rate limiting step in the photocyclic reaction sequence.[18] Oxygen formation is promoted *via* electron donation from the metal oxide to the transient $[Ru(bpy)_3]^{3+}$, hence periods of reduced light influx may allow the rate limiting step to proceed with self-decomposition of excess and unstable oxidized sensitizer minimized.

Therefore photocatalysis continued more efficiently for a sustained period, notably the drop away in reaction rate was observed to be offset for ~10 min with cyclic illumination (Fig. 3a).

Conclusions

$[Ru(bpy)_3]^{2+}$ has been extensively employed as the light harvester for photocatalytic water oxidations and is by far the most costly component of the reagent mixture. Thus any improvement of reaction efficiency with reduced sensitizer degradation is of interest. Furthermore, low cost abundant metal oxide catalysts with moderate surface area could be used effectively in these reactions as their activity, in terms of both reaction rate and duration, was enhanced by controlled lighting. We have recently investigated substitution of irreversible electron acceptor with an electron mediator.[20] A long term aim is the combining of these improvements for application and eventual implementation of water oxidation for storable solar fuels.

For this study the main mechanism for the enhanced yields is suggested to be from improved synchronization of the photocyclic reaction steps, which includes reduction in light sensitizer decomposition, balanced with maintaining the ongoing photoreaction with sufficient light influx. For use with natural sunlight, an oscillating prism system can be envisaged to

deliver the optimized fluctuating light intensity onto a reaction vessel.

$[Ru(bpy)_3]^{2+}$ is also increasingly being employed as photoredox agent in *e.g.* organic catalysis,[21–23] photopharmacology,[24] natural product synthesis,[25] and biochemical couplings such as C–S click reactions.[26] Thus effects of light source in terms of both wavelength and continuous *versus* fluctuating intensity has implications for these wider uses. Our further studies will include a detailed comparative study of light sensitizer decomposition rate and composition using spectroscopic analysis together with optimization of the cyclic illumination, including use with non-rare earth *e.g.* Zn-porphyrin light sensitizers.

Acknowledgements

We thank V. P. Ting and H. Doan UoBristol for assistance with BET analysis. DW and MTW acknowledge funding from a UoBath Faculty of Science departmental grant. S. R. H., J. P. and J. W. acknowledge the Engineering and Physical Sciences Research Council (EPSRC), UK (grant EP/G036780/1) and the Bristol Centre for Functional Nanomaterials for project funding.

Notes and references

1 S. Styring, *Faraday Discuss.*, 2012, **155**, 357–376.
2 Y. Tachibana, L. Vayssieres and J. R. Durrant, *Nat. Photonics*, 2012, **6**, 511–518.
3 K. J. Young, L. A. Martini, R. L. Milot, R. C. S. Iii, V. S. Batista, C. A. Schmuttenmaer, R. H. Crabtree and G. W. Brudvig, *Coord. Chem. Rev.*, 2012, **256**, 2503–2520.
4 C. Creutz and N. Sutin, *Proc. Natl. Acad. Sci. U. S. A.*, 1975, **72**, 2858–2862.
5 L. Duan, Y. Xu, P. Zhang, M. Wang and L. Sun, *Inorg. Chem.*, 2010, **49**, 209–215.
6 A. Harriman, G. Porter and P. Walters, *J. Chem. Soc., Faraday Trans. 2*, 1981, **77**, 2373–2383.
7 C. Herrero, A. Quaranta, W. Leibl, A. W. Rutherford and A. Aukauloo, *Energy Environ. Sci.*, 2011, **4**, 2353–2365.
8 M. Morikawa, Y. Ogura, N. Ahmed, S. Kawamura, G. Mikami, S. Okamoto and Y. Izumi, *Catal. Sci. Technol.*, 2014, **4**, 1644–1651.
9 D. Walsh, N. M. Sanchez-Ballester, V. P. Ting, S. R. Hall, L. R. Terry and M. T. Weller, *Catal. Sci. Technol.*, 2015, **5**, 4760–4764.
10 Q. Xiang, G. Chen and T.-C. Lau, *RSC Adv.*, 2015, **5**, 52210–52216.
11 T. K. Townsend, E. M. Sabio, N. D. Browning and F. E. Osterloh, *Energy Environ. Sci.*, 2011, **4**, 4270–4275.
12 A. Mishra and A. V. Malhotra, *J. Mater. Chem.*, 2009, **19**, 8528–8536.
13 R. A. Bepari, P. Bharali and B. K. Das, *J. Saudi Chem. Soc.*, DOI: 10.1016/j.jscs.2013.12.010.
14 D. Walsh, N. M. Sanchez-Ballester, K. Ariga, A. Tanaka and M. Weller, *Green Chem.*, 2015, **17**, 982–990.
15 F. Jiao and H. Frei, *Angew. Chem., Int. Ed.*, 2009, **48**, 1841–1844.
16 M. Hara, C. C. Waraksa, J. T. Lean, B. A. Lewis and T. E. Mallouk, *J. Phys. Chem. A*, 2000, **104**, 5275–5280.
17 A. Vaidyalingam and P. K. Dutta, *Anal. Chem.*, 2000, **72**, 5219–5224.
18 B. Limburg, E. Bouwman and S. Bonnet, *ACS Catal.*, 2016, **6**, 5273–5284.
19 P. K. Ghosh, B. S. Brunschwig, M. Chou, C. Creutz and N. Sutin, *J. Am. Chem. Soc.*, 1984, **106**, 4772–4783.
20 D. Walsh, N. M. Sanchez-Ballester, V. P. Ting, K. Ariga and M. T. Weller, *Catal. Sci. Technol.*, 2016, **6**, 3718–3722.
21 M. Oelgemoller and N. Hoffmann, *Org. Biomol. Chem.*, 2016, **14**, 7392–7442.
22 C. K. Prier, D. A. Rankic and D. W. C. MacMillan, *Chem. Rev.*, 2013, **113**(7), 5322–5363.
23 D. A. Nicewicz and D. W. C. MacMillan, *Science*, 2008, **322**, 77–80.
24 V. H. S. van Rixel, B. Siewert, S. L. Hopkins, S. H. C. Askes, A. Busemann, M. A. Siegler and S. Bonnet, *Chem. Sci.*, 2016, **7**, 4922–4929.
25 T. P. Nicholls, D. Leonori and A. C. Bissember, *Nat. Prod. Rep.*, 2016, DOI: 10.1039/c6np00070c.
26 S. S. Zalesskiy, N. S. Shlapakov and V. P. Ananikov, *Chem. Sci.*, 2016, DOI: 10.1039/c6sc02132h.

